EVOLUTION & DEVELOPMENT 13:5, 415–426 (2011)
DOI: 10.1111/j.1525-142X.2011.00500.x

Molecular anatomy of the developing limb in the coquí frog, *Eleutherodactylus coqui*

Joshua B. Gross,[a,1,*] Ryan Kerney,[b] James Hanken,[c] and Clifford J. Tabin[a]

[a] Department of Genetics, Harvard Medical School, Boston, MA 02115, USA
[b] Biology Department, Dalhousie University, Halifax, Nova Scotia, Canada B3H 4R2
[c] Museum of Comparative Zoology, Harvard University, Cambridge, MA 02138, USA

[*] Author for correspondence (email: joshua.gross@uc.edu)

[1] Current address: Department of Biological Sciences, University of Cincinnati, Cincinnati, Ohio 45221, USA

SUMMARY The vertebrate limb demonstrates remarkable similarity in basic organization across phylogenetically disparate groups. To gain further insight into how this morphological similarity is maintained in different developmental contexts, we explored the molecular anatomy of size-reduced embryos of the Puerto Rican coquí frog, *Eleutherodactylus coqui*. This animal demonstrates direct development, a life-history strategy marked by rapid progression from egg to adult and absence of a free-living, aquatic larva. Nonetheless, coquí exhibits a basal anuran limb structure, with four toes on the forelimb and five toes on the hind limb. We investigated the extent to which coquí limb bud development conforms to the model of limb development derived from amniote studies. Toward this end, we characterized dynamic patterns of expression for 13 critical patterning genes across three principle stages of limb development. As expected, most genes demonstrate expression patterns that are essentially unchanged compared to amniote species. For example, we identified an *EcFgf8*-expression domain within the apical ectodermal ridge (AER). This expression pattern defines a putatively functional AER signaling domain, despite the absence of a morphological ridge in coquí embryos. However, two genes, *EcMeis2* and *EcAlx4*, demonstrate altered domains of expression, which imply a potential shift in gene function between coquí frogs and amniote model systems. Unexpectedly, several genes thought to be critical for limb patterning in other systems, including *EcFgf4*, *EcWnt3a*, *EcWnt7a*, and *EcGremlin*, demonstrated no evident expression pattern in the limb at the three stages we analyzed. The absence of *EcFgf4* and *EcWnt3a* expression during limb patterning is perhaps not surprising, given that neither gene is critical for proper limb development in the mouse, based on knockout and expression analyses. In contrast, absence of *EcWnt7a* and *EcGremlin* is surprising, given that expression of these molecules appears to be absolutely essential in all other model systems so far examined. Although this analysis substantiates the existence of a core set of ancient limb-patterning molecules, which likely mediate identical functions across highly diverse vertebrate forms, it also reveals remarkable evolutionary flexibility in the genetic control of a conserved morphological pattern across evolutionary time.

INTRODUCTION

Despite great phylogenetic breadth, often accompanied by extensive differences in life history and functional anatomy, all vertebrates retain a shared, underlying body plan. For example, essential features of the tetrapod limb, such as basic skeletal and muscle patterns, remain recognizable even as the limb has been modified for uses as divergent as the flying wing of a bat or the swimming flipper of a whale (a phenomenon Darwin correctly identified as an example of homology, or similarity by common descent). Developmental biologists frequently assume that the conserved morphological features of the tetrapod limb reflect conservation of the basic core genetic modules that organize the embryonic limb bud, even as modifications to the genetic circuitry at later developmental stages modify the ultimate form of the limb in key ways. This assumption is very powerful, insofar as it allows one to extrapolate from the combined data set generated with complementary model systems, such as chicken and mouse. Indeed, it underlies the belief that, although secondary modifications undoubtedly occur over evolutionary time, the key genetic processes that establish the basic framework by which the limb forms are conserved. Evidence for this assumption, however, has largely been inferred from studies of amniotes. To evaluate its validity over a larger phylogenetic distance, we turned to the developing limb bud of the tiny embryos of the Puerto Rican frog, *Eleutherodactylus coqui*.

Coquí frogs are a model system for the study of direct development, a life-history strategy marked by rapid development from egg to adult and absence of a free-living, aquatic larva (Elinson and Beckham 2002). In contrast to metamorphic anurans, coquí frogs develop numerous adult

anatomical features rapidly in the egg, prior to hatching as miniature adults. In this way, this species demonstrates heterochrony, a rapid and early development of morphological features compared to metamorphic anurans, which retain the ancestral, bi-phasic life-history condition (Schlosser 2001).

Perhaps the most conspicuous heterochronic trait is the limb, which in coquí emerges shortly after neurulation—coincident with somite development—instead of during later larval development as in most amphibians (Townsend and Stewart 1985; Richardson et al. 1998). Early developmental studies explored the capacity for explanted coquí limbs to develop autonomously in culture, or following transplantation to juvenile metamorphic hosts (Elinson 1994). Subsequent studies have begun to focus on the extent to which coquí adheres to the model of limb development defined by studies in chicken and mouse (Hanken et al. 2001). These investigations reveal notable morphological differences, including the observation that hind limb buds are larger and more developed than forelimb buds throughout embryogenesis, and the emergence of early limb buds that appear "detached" from the primary axis of the body (Richardson et al. 1998; Hanken et al. 2001). There also are changes in the timing of some of the later steps of limb morphogenesis. For example, Kerney and Hanken (2008) recently reported distal domains of expression of the skeletal markers *Runx2* and *Sox9* in coquí prior to formation of the proximal skeletal condensations. This precocious expression pattern represents a significant departure from the conserved proximal-to-distal temporal gradient that is characteristic of limb morphogenesis in amniote models (Kerney and Hanken 2008).

For the most part, however, morphogenesis of the limb in coquí is very similar to that in amniotes. Thus, coquí limbs display similarities in the fundamental sequence and pattern of limb chondrogenesis, proceeding proximodistally from pelvic and pectoral girdles to phalanges (Hanken et al. 2001). Digit formation proceeds in a posterior-to-anterior sequence similar to amniotes, a pattern conserved among tetrapods with the exception of urodeles.

Given this apparent conservation of both the process of limb formation and the structure that is produced, it is not surprising that (to the extent it has been examined) molecular patterning of the early limb seems to follow the same script in coquí as in amniotes. For example, *Raldh2* plays a critical role in forelimb bud initiation across Osteichthyes and is expressed in a domain suggestive of a similar role in the early coquí forelimb field (Elinson et al. 2008). During this phase, *Pitx1* expression in the hind limb field is important for establishing a discrete hind limb identity (Logan and Tabin 1999) and *Pitx1* expression in the developing hind limb is conserved in coquí. Unique expression is also detected in a sub-region of the forelimb, a domain not observed in other taxa (Chang et al. 2006). Sabo et al. (2009) investigated another widely expressed and highly conserved gene, *Lbx1*, in the context of coquí limb development. They demonstrate that *Lbx1*-expressing cells likely migrate from the somite into the limb bud to form muscle (Sabo et al. 2009). Another gene family known to be important for limb outgrowth, in tetrapods as well as in all appendage-bearing animals, is the *Dlx* genes (Panganiban et al. 1997). Indeed, expression of *Dlx* mRNA (*EcDlx2* and *EcDlx4*; Fang and Elinson 1996) and protein (Hanken et al. 2001) has been observed in the coquí distal ectoderm, as it is in amniotes.

Once the limb bud has formed, according to amniote models, limb patterning along proximodistal and anteroposterior axes is under the control of two key signaling centers, the apical ectodermal ridge (AER) and the zone of polarizing activity (ZPA), respectively. Both centers have been studied to some extent in coquí. There is no morphological structure resembling the AER in the coquí limb bud (Hanken et al. 2001). However, this is not really an issue in terms of molecular patterning as it is well known that many amphibians including the frog *Xenopus laevis* also lack a morphological AER, but there is a distinct stripe of gene expression in *Xenopus* where the key proximodistal patterning gene *Fgf8* is expressed in the proper location (Christen and Slack 1997). Also, excision of the distal ectoderm in coquí does not lead to proximodistal limb truncation but rather to defects of the skeletal pattern, as in avian species (Richardson et al. 1998). However, the truncations following AER removal in chicken reflect an apoptotic response to the surgery and are not indicative of patterning mechanisms (Dudley et al. 2002).

Although there is scant evidence for conservation of an AER signaling center in coquí, there are no data against it either. In contrast, there is direct evidence that the ZPA is present in coquí and that it plays an equivalent role in patterning the anterior–posterior axis in this species, as in amniotes. The posterior presumptive ZPA tissue of the coquí limb bud has the ability to induce extra digits following transplantation to the anterior bud as in chicken embryos (Hanken et al. 2001). Moreover, the gene encoding the key ZPA morphogen, Sonic hedgehog (Shh), is expressed in an equivalent spatial pattern (Hanken et al. 2001). Whereas coquí limb buds display an earlier cessation of the inductive ability of the ZPA compared to chicken and a concomitant relatively shorter period of *EcShh* expression compared to amniotes (Hanken et al. 2001), this represents a shift in the timing of its action (heterochrony) but not its role. Although as previously observed, the coquí limb develops as a modular structure bearing a mosaic of conserved and derived features (Hanken et al. 2001), the core patterning mechanisms appear to be conserved. This is consistent with the common bauplan of the limb in all tetrapods. Nonetheless, this conclusion is based on a fairly limited set of comparisons. In this report, we extend earlier analyses by focusing on a panel of genes that are regarded as essential molecular regulators of limb bud development. We present the results of our expression

and timing analyses across three critical stages of limb development in coquí: early outgrowth (TS 5), digital "pad" stage (TS 6/7), and prehatching (TS 8). We compare our results with those described in amniotes and identify surprising differences in several core components of the limb-patterning system.

MATERIALS AND METHODS

Collection of live animals

Live animal collection permits were obtained from the Department of Natural and Environmental Resources in Puerto Rico (DRNA no. 06-IC-025) and the Caribbean National Forest (no. CNF-2082; USDA Forest Service). Field collections were carried out in May 2007 at the Luquillo Experimental Forest, El Yunque National Forest.

Thirty sexually mature adults (15 male, 15 female) and 120 embryos were collected on the grounds near the El Verde Research Station at El Yunque. Adults were collected near trees or in forest leaf litter shortly after dusk. Adults were fed and maintained in moist 4-oz containers and shipped live in IATA-approved storage containers from San Juan to Boston using an overnight courier service (World Courier, Inc., New Hyde Park, NY, USA). Adults were then maintained as a breeding colony in humidity- and temperature-controlled chambers at the Hanken lab (Harvard University).

Clutches of embryos were collected from closed palm fronds in forest leaf litter at varying times of day. Embryos were fixed in either 4% paraformaldehyde or MEMFA fixative. Embryos used in this study included wild-caught embryos, embryos derived from our breeding colony, and embryos derived from the breeding colony maintained in the Elinson lab (Duquesne University). Following fixation overnight at 4°C, or 1 h at room temperature, embryos were transferred to 100% methanol for storage at −20°C prior to histological processing.

Cloning and characterization of gene fragments

Total RNA was isolated from embryonic and adult tissue using Trizol reagent (Invitrogen) and processed according to manufacturer's instructions. cDNA preparations were generated from pooled RNA using the Roche Transcriptor RNA kit (Roche). Degenerate polymerase chain reaction PCR primers were designed to conserved amino acid residues within the coding sequence of numerous genes (see below) using the online software tool, CODEHOP (Rose et al. 2003).

The following degenerate primers pairs were used to amplify gene fragments of interest in this study: *EcMeis2*- forward (5′-TGCTCTGAAAAGAGATAAAGATGCTATHTAYGGNCA-3′), *EcMeis2*-reverse (5′-CCTGAGACACAGCTCTATTAGACTGATCDATCATNGG-3′); *EcBmp4*-forward (5′-GCTTCTAGAGCTAATACAGTGTGTTCTTTYCAYCAYGARG-3′), *EcBmp4*-reverse (5′-CCACATCCTTCCACCACCATRTCYTGRTA-3′); *EcWnt7a*-forward (5′-ATTATTGCTGCTGGAGTGGCNCAYGCNAT-3′), *EcWnt7a*-reverse (5′-TCTAGAATACTGATGTGTATTATATCCTCTTCCRCARCACAT-3′); *EcFgf8*-forward (5′-ACAGATCAGCTGTCTAGAAGACTGATTMGNACNTAYCA-3′), *EcFgf8*-reverse (5′-GTCTTCCTTTTCTTGTAAAAGCCATRWACCA-3′); *EcWnt5a*-forward (5′- GAGCTAAAACAGGAATTAAAGAATGTCARTAYCARTT-3′), *EcWnt5a*-reverse (5′-CTTTTTACATTTCACATAACAACACCARTGRAA-3′); *EcFgf4*-forward (5′-TGGGAATTAAAAGACTGAGAAGACTGTAYTGYAAYGT-3′), *EcFgf4*-reverse (5′-GGCAGAAAATGTGTCAGTGTCATNGTNGG-3′); *EcLmx1b*-forward (5′-TGTGTGTATCATCTGAGTTGTTTTTGYTGYTGYGT-3′), *EcLmx1b*-reverse (5′-AAAATAAGAAGACTGCATAGAATACAGTCTATCDATNGGRTT-3′); *EcHand2*-forward (5′-TCTCTGGTGGGAGGATTTCCNCAYCAYCC-3′), *EcHand2*-reverse (5′-GCCATCCTGTTCTTCCTTTTGTYTTYTTRTC-3′); *EcGremlin*-forward (5′-GATCTCAGGGAGCTATTCCACCNCCNGAYAA-3′), *EcGremlin*-reverse (5′-TTGTTGGTGGCTGCAGTTCNGGRCARTT-3′); *EcWnt3a*-forward (5′-GGAGTGAAAATTGGAATTCAGGARTGYCARCA-3′), *EcWnt3a*-reverse (5′-CATCCATCAATTCCATGAGATGTNACRTTRCA-3′); *EcAlx4*-forward (5′-GAATCTAATAAAGGCAAGAAAAGAAGAAAYMGNACNAC-3′), *EcAlx4*-reverse (5′-GCTCTTGTCAGCAGTGGCARYTCRTANGC-3′); *EcPtch1*-forward (5′-CCACTGGATTGTTTTTGGGARGGNGC-3′), *EcPtch1*-reverse (5′- CAGTTCTTCCTGCCAATGCATRTAYTT-3′). Gene fragments were isolated using the following gradient PCR program: (1) 94°C for 5 min; (2) 94°C for 45 sec; (3) 48–66°C for 45 sec; (4) 72°C for 90 sec; (5) repeat steps 2–4, 34 times; (6) 72°C for 5 min; (7) final step cooled to 4°C.

Amplified PCR fragments were gel-purified and subcloned into the pGEM-T Easy vector (Promega) using DNA ligation kit version 2.1 (Takara). Ligation reactions were then transformed to approximately 100 μl of competent DH5α *Escherichia coli* cells. Transformants were plated on ampicillin-resistant, blue/white selection agar plates overnight at 37°C. Multiple white colonies were isolated and grown overnight in ampicillin-resistant LB broth and prepared for sequencing.

In situ hybridization

RNA probe templates were generated by PCR in which gene fragment inserts were amplified using M13F and M13R primers. Probe was synthesized using the following reagents: 10.5 μl dH_20-DEPC, 2 μl 10× Nucleotide Digoxigenin-labeling mix (Roche), 4 μl template, 0.5 μl RNAse Inhibitor (Roche), and 1 μl of RNA Polymerase (Roche). The reaction was incubated for 2 h at 37°C. The reaction was ended with the addition of 1 μl DNAse (RNAse-free; Roche) for 15 min at 37°C. Probe was then precipitated, washed with sterile 100% EtOH, resuspended in 50 μl of dH_2O-DEPC, and stored at −80°C.

On day 1, coquí embryos were rehydrated from MeOH in a series of 10-min incubations in 75% MeOH/PBT (PBS + 0.1% Tween-20), 50% MeOH/PBT, 25% MeOH/PBT, and incubated for approximately 15 min in 100% PBT. Embryos were then treated with Proteinase K (10 mg/ml; Roche) at a dilution of 1:1000 for 15 min at room temperature to facilitate probe

binding. Following Proteinase K treatment, embryos were refixed in a solution of 4% paraformaldehyde/2% gluteraldehyde/PBT. Following a series of rinses in PBT, embryos were transferred to scintillation vials with prewarmed hybridization solution and incubated at 70°C for 1 h. We then replaced fresh hybridization solution to each vial and added 10 μl of RNA probe and incubated overnight at 70°C in a shaking water bath.

On day 2, embryos were rinsed in prewarmed Solution I (50% formamide/2× SSC [pH 4.5]/1% SDS) for 30 min in a 70°C water bath. Embryos were rinsed over the next 6 h in fresh Solution 1, in a set of six 30-min incubations. Embryos were then incubated in a 1:1 mixture of Solution I and MABT solution (100 mM Maleic acid; 150 mM NaCl; 0.1% Tween-20; pH 7.5). Following three rinses and 3 × 30 min incubations, embryos were transferred to a solution of 20% heat-inactivated normal goat serum (HINGS) + 2% blocking reagent (BR; Roche) in MABT solution. After an hour of incubation at room temperature, fresh HINGS/BR/MABT solution was replaced to each vial with the addition of a 1:2000 dilution of α-digoxigenin-AP (Roche).

On day 3, embryos were rinsed all day in MABT solution at room temperature. Fresh solution was replaced to each vial at least once an hour. Vials were incubated overnight at 4°C in MABT.

On day 4, embryos were rinsed in NTM solution (100 mM NaCl; 100 mM Tris [pH 9.5]; 50 mM $MgCl_2$) for a series of 4 × 10 min washes at room temperature. Vials were then replaced with 1 ml of NTM with 4.5 μl NBT and 7 μl BCIP. Vials were wrapped in aluminium foil and allowed to develop in the dark between 15 min and several hours (depending on the probe). Once staining was complete, embryos were rinsed twice in PBT and transferred to a solution of TBST (TBS + 0.1% Tween-20). All stained embryos were then stored in 4% paraformaldehyde at 4°C.

In total, 176 embryos were assessed in this study for each of 13 genes over three developmental stages (TS 5, 6/7, and 8). Each stage was assessed at least three times for a given gene over the course of six different experiments. All images presented are representative of the gene expression pattern observed among individuals. In embryos that did not demonstrate expression following in situ analysis, it is formally possible that our probes did not work, or that the stringency of our preparation and protocol was not optimal.

Gene fragment analysis

Plasmids were sequenced by the Dana Farber/Harvard Cancer Center Sequencing facility, using the M13F and M13R universal primer sites. Raw sequence files were aligned using SeqMan (DNAStar Lasergene). Annotated fragment sequences were analyzed, identified, and named according to their strongest returned E values (by consensus) using the BlastX (NCBI) search tool (Table 1). We present the percent similarity of each sequence to the top three hits returned in our analysis. We sought to determine whether any of our sequences might actually represent a paralogous or related gene family member. To that end, we selected any sequence in the top 100 returned hits that departed from the gene name assigned. These "alternative identities" are listed, along with the maximum percentage identity to the organism from which the sequence is derived, in Table 1 ("Alternative identities"). In every case, the alternative identity is lower than all top three hits for each sequence (Table 1).

Of the genes we identified, only *Alx4* has not been characterized or accessioned to public databases for *X. laevis*. All gene sequences have been deposited to the NCBI database.

Imaging

Whole-mount individual specimens were imaged using a Leica MZ FLIII stereomicroscope. Photomicrographs were collected using the ACT-1 software package and processed using Adobe Photoshop CS3.

RESULTS AND DISCUSSION

We examined in the coquí limb bud the expression patterns of a number of genes believed to play key roles in the patterning of the three cardinal axes of the amniote limb bud. Reflecting the conserved organization of all tetrapod limbs, many of the genetic modules that regulate each axis in higher vertebrates are expressed in domains consistent with their having equivalent roles in coquí. However, surprising differences emerged as well, indicating that these fundamental regulatory genetic cassettes may be more evolutionarily labile than is generally appreciated.

The anterior–posterior axis

Shh is a secreted protein that mediates the polarizing activity of the ZPA (Riddle et al. 1993). Embryonic expression of *EcShh* in coquí has already been demonstrated (Hanken et al. 2001). We verified this expression and characterized the dynamic expression of *EcShh* over the course of three critical stages in limb bud development (Fig. 1, A–F). Early expression in the forelimb is weak (Fig. 1A), with stronger expression in the hind limb (Fig. 1D). This result is unsurprising given the conserved expression pattern (and presumed function) of *Shh* across vertebrates (Marigo et al. 1996b). The most obvious expression domains in the forelimb (Fig. 1B) and hind limb (Fig. 1E) buds were observed at TS 6/7 within a restricted domain approximating the ZPA. By TS 8, *EcShh* expression is essentially absent from the limb buds (Fig. 1, C and F), with only minimal expression observed in the apical ridge of the tip of the limb. This expression, however, was observed only in the hind limb bud (Fig. 1F).

Patched1 (Ptch1) is the receptor for Shh (Marigo et al. 1996a; Stone et al. 1996). In addition, *Ptch1* is strongly upregulated in response to Shh signaling (Goodrich et al. 1996; Marigo et al. 1996c), thereby limiting ligand diffusion. The direct upregulation of *Ptch1* by Shh is a conserved feature,

Table 1. BLASTX sequence similarity of DNA fragments isolated from *Eleutherodactylus coqui*

Gene sequence	Fragment size	Amino acid percent similarity	
		Top three hits[1]	Alternative identities
EcBmp4	869 bp	98%/90%/89%	*Bmp2* (65%; *Gallus*)
EcHand2	596 bp	97%/96%/93%	*Hand1* (50%; *Xenopus*)
EcPtch1	368 bp	80%/80%/80%	*Ptch2* (73%; *Danio*)
EcFgf8	404 bp	93%/93%/91%	*Fgf17* (72%; *Danio*)
EcWnt5a	824 bp	96%/95%/93%	*Wnt5b* (84%; *Gallus*)
EcLmx1b	782 bp	96%/95%/93%	*Lmx1a* (68%; *Monodelphis*)
EcAlx4	581 bp	90%/86%/86%	*Alx1* (57%; *Sus*)
EcMeis2	791 bp	99%/89%/89%	*Meis1* (81%; *Oryctolagus*)
EcFgf4	386 bp	77%/69%/68%	*Fgf6* (64%; *Danio*)
EcWnt7a	623 bp	90%/90%/90%	*Wnt7b* (76%; *Xenopus*)
EcWnt3a	701 bp	97%/93%/93%	*Wnt4* (50%; *Equus*)
EcGremlin	440 bp	99%/99%/98%	*Gremlin2* (75%; *Ictalurus*)

[1]Values indicate the percent amino acid similarities for the top three hits of a BlastX search of each coquí fragment isolated in this study. The coquí fragment was named based on the consensus identity derived from this search.

not just during limb development, but also in all known examples of hedgehog signaling. Not surprisingly, *EcPtch1* expression in coquí overlaps with and extends beyond the domains of *EcShh* in the coquí limb bud as it does in other vertebrates. In TS 5 coquí embryos, *EcPtch1* is expressed in the posterior portion of the forelimb and hind limb buds (Fig. 1, G and J), but with only minimal expression in the forelimb bud (Fig. 1G). Subsequently, the pattern of *EcPtch1* expression continues to parallel and extend beyond that of Shh. At TS 6/7, *EcPtch1* remains confined to distal portions of the limb buds (Fig. 1, H and K). By TS 8, *EcPtch1* expression diminishes from both limbs (Fig. 1, I and L), but in the hind limb, this expression expands to encompass the distal half of the developing limb bud (Fig. 1L).

Given the importance of Shh in anteroposterior limb patterning, it is not surprising that there is a complex network of upstream genes that positively regulate its initial expression in the posterior limb bud (e.g., *Hand2*, *HoxD13*, *Tbx2/3*—Zakany and Duboule 1996; te Welscher et al. 2002; Suzuki et al. 2004) and negatively regulate its expression anteriorly (e.g., *Twst1*, *Alx4*, *Gli3*—Dunn et al. 1997; Qu et al. 1997; Bourgeois et al. 1998; Zhang et al. 2009). We examined the expression of one positively acting and one negatively acting member of this regulatory system.

In amniotes, *Hand2* plays an essential role in "pre-patterning" the limb bud through establishment of the Shh signaling center within the posterior mesenchyme (te Welscher et al. 2002). As such, *Hand2* is critical for generating the anterior–posterior polarization of the limb (Charite et al. 2000; Fernandez-Teran et al. 2000; te Welscher et al. 2002). In coquí embryos, as in amniotes, early expression of *EcHand2* in the limb bud is limited to a posterior domain that extends beyond the limit of *EcShh* expression within the ZPA. The domain of expression, early in limb development, is reduced in the forelimb (Fig. 1M) compared to the hind limb (Fig. 1P). This reduced level of forelimb expression continues into TS 6/7 when *EcHand2* expression expands from the most proximal aspect of the developing limb to its most distal tip (Fig. 1N). This expression pattern remains confined to the posterior half of the limb bud, with the exception of a small anteriorly extended domain of expression within the mid-digital pad (Fig. 1Q). By TS 8, expression of *EcHand2* begins to diminish from the proximal region of both limb buds (Fig. 1, O and R), following a similar pattern of expression observed in amniotes (Fernandez-Teran et al. 2000). In contrast to chicken, however, *EcHand2* expression is not observed at the periphery of developing digital cartilages. The timing of expression of *EcHand2* is delayed in the forelimb (Fig. 1M) compared to the hind limb (Fig. 1P) across the observed developmental stages.

Alx4 encodes the paired-related, homeobox protein aristaless-like four protein (Qu et al. 1999). In amniotes, this protein is expressed in anterior limb bud mesenchyme, but it is excluded from posterior mesenchyme by *Hand2* (McFadden et al. 2002). Alx4 protein acts as a transcriptional repressor, contributing to determination of antero-posterior positional identity of the limb bud by restricting ZPA formation to the posterior limb bud (Qu et al. 1997). In coquí, *EcAlx4* is very faintly expressed in the forelimb bud at TS 5 (Fig. 1S), with a slight anterior bias. Expression in the hind limb (Fig. 1V) similarly is very faint and diffuse. By TS 6/7, stronger anterior expression is confined to the medial "bulge" of the forelimb (Fig. 1T). In contrast, the hind limb demonstrates both

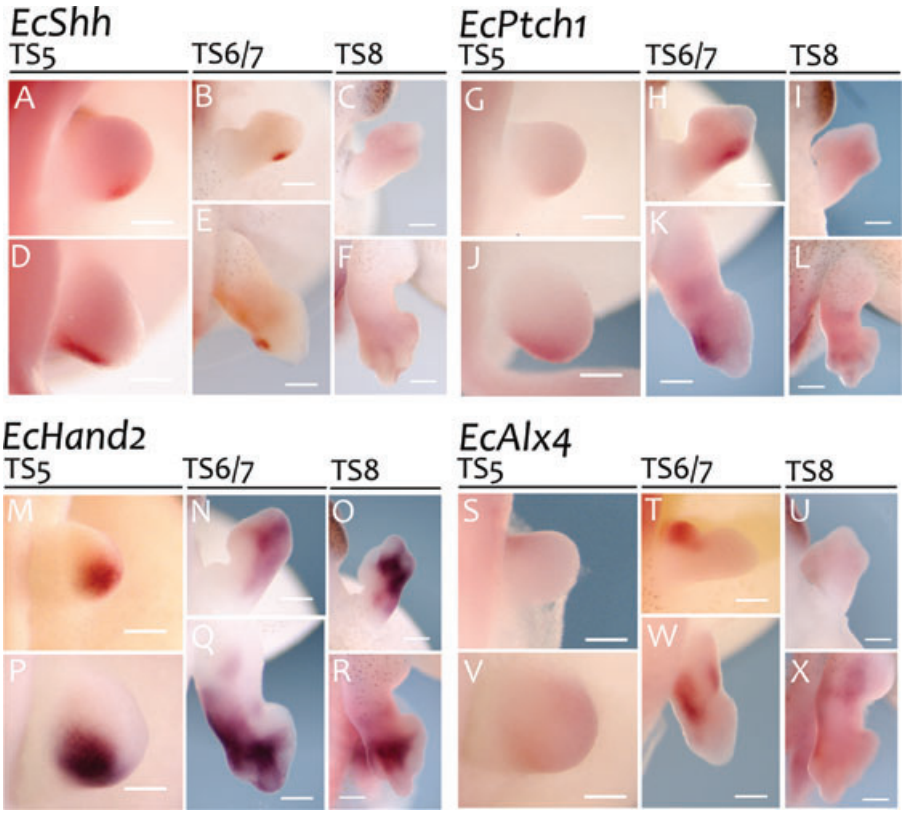

Fig. 1. Analysis of *EcShh*, *EcPtch1*, *EcHand2*, and *EcAlx4* in coquí limb buds reveals conserved patterns of gene expression compared to amniotes. Early expression of *EcShh* is weak in the forelimb (A), with somewhat stronger expression in the hind limb (D). By TS 6/7, *EcShh* is clearly present in the zone of polarizing activity (ZPA) of both the forelimb and hind limb (B and E). By TS 8, *EcShh* is absent from the entire limb bud except for a small amount of expression in the apical tip of the hind limb (C and F). *EcPtch1* expression is absent from the forelimb at TS 5 (G), with nascent expression in the ZPA of the hind limb (J). The domain of *EcPtch1* expression extends beyond that of *EcShh* at TS 6/7 (H and K), but by TS 8 *EcPtch1* expands to the distal half of the limb bud (I and L). The transcription factor *EcHand2* is restricted to the posterior limb bud near the ZPA at TS 5 (M and P). This posterior restriction continues through TS 6/7, becoming weaker in the forelimb compared to the hind limb (N and Q). By TS 8, *EcHand2* expression diminishes from the most proximal region of the limb (O and R). At TS 5, *EcAlx4* is faintly expressed in both forelimb (S) and hind limb (V), with a slight anterior bias. At TS 6/7 expression becomes stronger in both limbs (T and W). Expression in the forelimb at this stage is confined to the median "bulge" in the anterior portion of the developing limb (T). Interestingly, *EcAlx4* expression in the hind limb at stage TS 6/7 is present as anterior and posterior "stripes," with a larger domain of expression in the posterior limb (W). By TS 8, *EcAlx4* expression is essentially absent from the forelimb (U). At this stage, the hind limb retains both anterior and posterior domains of expression, albeit greatly reduced compared to TS 6/7 (X). Forelimbs: A–C, G–I, M–O, S–U; hind limbs: D–F, J–L, P–R, V–X. Scale = 250 μm.

anterior and posterior domains of expression (Fig. 1W), which represent a distinct departure from the anteriorly confined expression observed in amniotes (te Welscher et al. 2002). At later stages, expression of *EcAlx4* is essentially absent from the forelimb (Fig. 1U). In TS 8 hind limbs, anterior and posterior domains of expression persist but are greatly reduced in intensity (Fig. 1X). Although there are differences in the details of the expression of this gene in coquí relative to amniotes, the expression pattern is consistent with a conserved role in the regulation of Shh during the initiation phase.

The proximodistal axis

The key secreted proteins that drive outgrowth and patterning of the proximodistal limb axis are members of the fibroblast growth factor (Fgf) family, which in amniotes are expressed in the AER, a specialized pseudo-stratified epithelium at the distal tip of the limb bud. As noted above, and as in other anurans, including *X. laevis*, coquí lacks this morphological structure. However, past studies have demonstrated a region of thickened ectoderm along the apex of the growing limb bud (Richardson et al. 1998). Given the importance of Fgf activity in limb development and the expression of *Fgf8* in a stripe at the distal end of the *Xenopus* limb bud despite absence of an AER, it was expected that *Fgf* genes would be expressed similarly in coquí.

Four *Fgf* family members are expressed in the mouse AER; *Fgf4*, *8*, *9*, and *17*. Mutational analysis indicates that Fgf8 is the most critical of these for limb bud initiation and outgrowth (Lewandoski et al. 2000). Indeed, as anticipated, expression of *EcFgf8* is evident within an apical region of distal ectoderm that is equivalent to the AER (Fig. 2, A–J). We also examined the expression of *EcFgf4*, a second member of the *Fgf* family that is expressed in the AER of amniotes. The *EcFgf4* probe did not reveal transcription of *EcFgf4* in the limb AER at any stage analyzed (Fig. 2, K-M). It must be noted, however, that *Fgf4* is expendable during mouse limb development (Sun et al. 2000), presumably due to genetic redundancy with other Fgf family members.

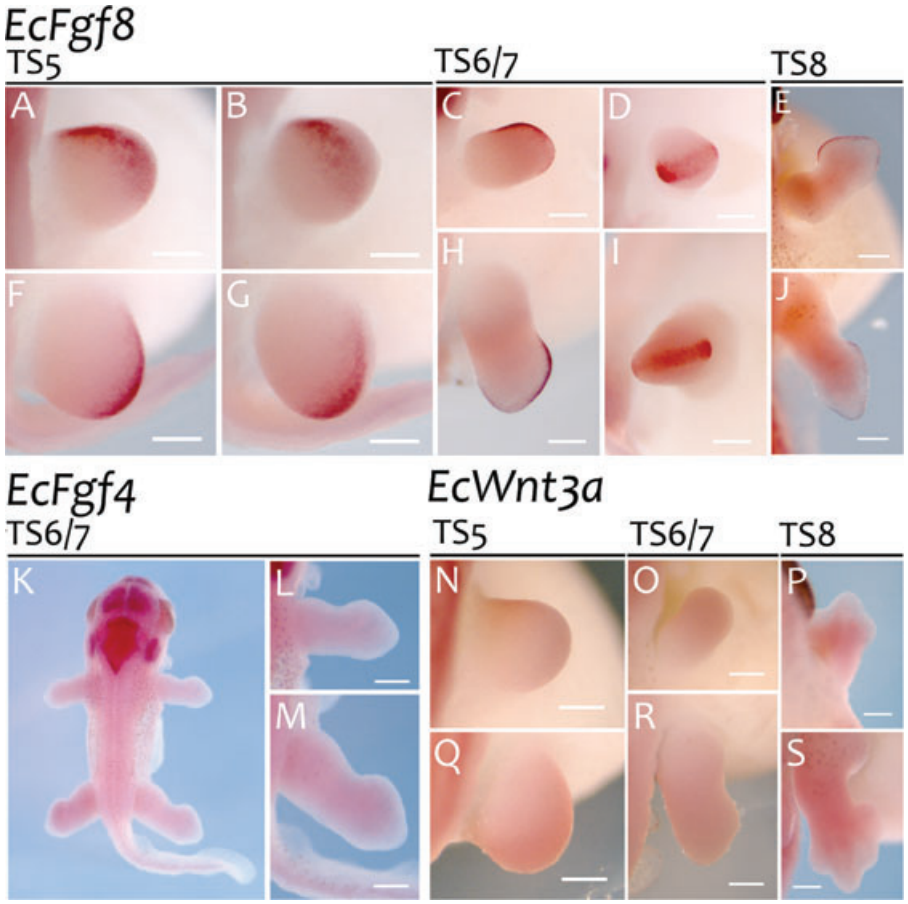

Fig. 2. *EcFgf8*, *EcFgf4*, and *EcWnt3a* expression in coquí limb buds. *EcFgf8* is strongly expressed in the region that corresponds to the AER through all stages of development analyzed in both forelimb (A–E) and hind limb (F–J). Expression of *EcFgf8* appears to be strongest within the region of thickened ectoderm in the distal developing limb (Richardson et al. 1998). The gene *EcFgf4* was assayed through all stages of development (data not shown) but was not expressed in any tissue-specific manner (K–M). We did observe, however, some chromogen "trapping" in the ventricles of the brain and otic capsules (K) of specimens exposed for extended periods of time. No expression was detected for *EcWnt3a* (N–S) in any embryo throughout the three stages assayed. Forelimbs: A–E, L, N–P; hind limbs: F–J, M, Q–S. Scale = 250 μm.

Our results with coquí indicate that it may be expendable evolutionarily as well.

In the developing chicken limb, a key gene acting upstream, initiating Fgf signaling, is the canonical Wnt family member *Wnt3a*. *Wnt3a* is expressed early in the presumptive AER where it induces expression of *Fgf8* via the canonical β-catenin signaling pathway and thereby promotes AER formation (Kengaku et al. 1998). Subsequently, *Wnt3a* is expressed within the AER itself, initiating *Fgf* expression. However, *EcWnt3a* is not observed at any point during development of coquí limb buds (Fig. 2, N–S). Absence of *EcWnt3a* expression in the developing coquí limb may indicate that a different Wnt family member fulfills the role of this gene in inducing the expression of *EcFgf8* in this species. Consistent with this idea, *Wnt3a* is not expressed in the forming mouse AER and is unnecessary for either *Fgf8* expression or AER formation. Instead, a different canonical Wnt, *Wnt3*, is expressed in the early distal ectoderm and plays exactly these roles in the mouse (Barrow et al. 2003). This surprising finding demonstrates that two family members with identical signaling properties can substitute for one another over evolutionary time, even though they are not expressed together in a redundant fashion in any known species.

One of the key genes involved in proximodistal axis formation downstream of Fgf activity is *Wnt5a*, which is expressed in the underlying distal mesenchyme of the developing limb (Dealy et al. 1993). *Wnt5a* is essential for the growth but not the patterning of proximodistal limb structures (Yamaguchi et al. 1999). As in amniotes, expression of *EcWnt5a* in early coquí limb buds remains largely diffuse with a slight distal bias (Fig. 3, A and D). This distal expression pattern becomes more distinct later in development, becoming more pronounced in the digital pad by stages TS 6/7 (Fig. 3, B and E). By TS 8, expression in the mature limb bud is confined to portions of the developing digits as they grow out from the primary limb axis (Fig. 3, C and F). We observe a similar reduction in expression around the digits of the hind limb, as observed in the chicken (Kawakami et al. 1999). However, and in contrast to several gene expression patterns, we do not observe a delay in expression of *EcWnt5a* in the forelimb compared to the hind limb. Instead, expression of *EcWnt5a* in both limb buds proceeds at roughly the same pace in all four limbs.

One of the roles of Fgf activity in limb patterning is to repress expression of the homeodomain transcription factors *Meis1* and *Meis2* in distal limb mesenchyme. These closely

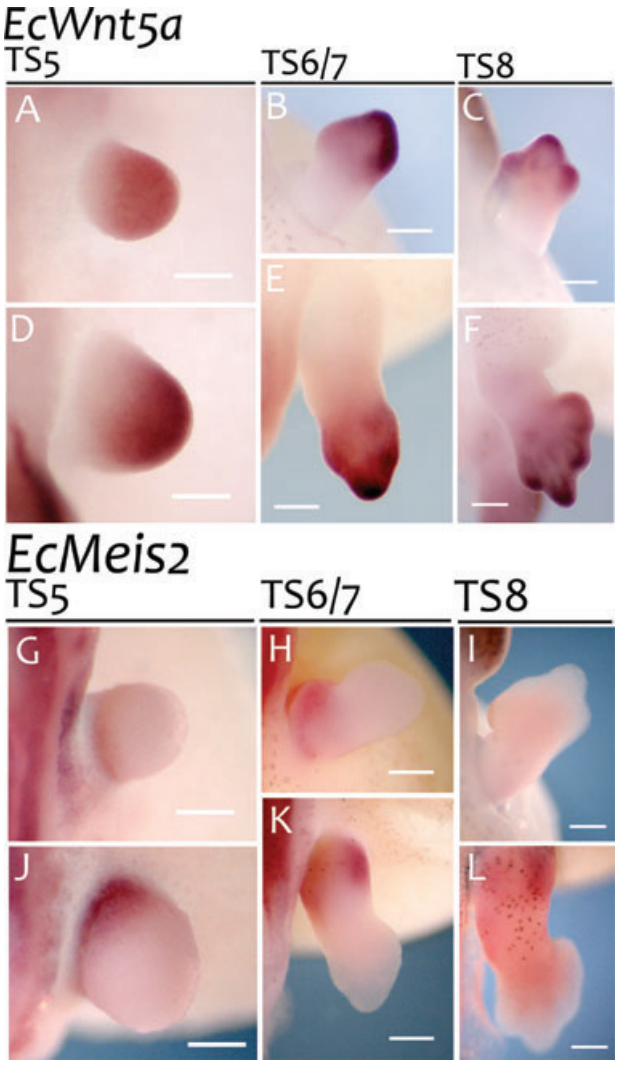

Fig. 3. Expression patterns of *EcWnt5a* and *EcMeis2* in coquí limb buds. *EcWnt5a* is expressed in a largely diffuse pattern in the early forelimb (A), with a bias of stronger expression distally as in the hind limb (D). Distal expression of *EcWnt5a* becomes more intense by *TS* 6/7 (B and E). At TS 8, expression is localized to the distal region in both forelimb and hind limb, as in amniotes (C and F). *EcMeis2* expression is faint in the forelimb of TS 5 embryos (G), with stronger expression in the hind limb (J). Note the anterior bias of expression in the hind limb at this stage. At TS 6/7, expression becomes stronger in both the forelimb (H) and hind limb (K) but remains confined to anterior and proximal aspects of each limb. At TS 8, *EcMeis2* expression is lost from the forelimb (I). In the hind limb, *EcMeis2* expression appears diffuse throughout the limb bud, with strongest staining observed in the anterior aspect (L). Forelimbs: A–C, G–I; hind limbs: D–F, J–K. Scale = 250 μm.

related homeobox transcription factors (Cecconi et al. 1997) function similarly during limb development. For instance, overexpression of either *Meis1* or *Meis2* yields the same distal limb truncation phenotype (Capdevila et al. 1999; Mercader et al. 1999). *Meis2* is involved in the specification of proximal elements of the developing limb (Mercader et al. 2000). As in amniotes, *EcMeis2* expression in coquí is also restricted to the most proximal domain of the embryonic limb. However, unlike the expression domains previously described for this gene, in coquí there is a distinct anterior bias. We detected faint *EcMeis2* expression in the TS 5 coquí forelimb (Fig. 3G), with weak expression observed in the most proximal margin. Expression is more pronounced in the hind limb bud at TS 5, but it is biased anteriorly (Fig. 3J). Stronger expression is observed in the proximal region of the limb bud at TS 6/7, but in both forelimb (Fig. 3H) and hind limb (Fig. 3K) buds, this expression continues to have an anterior bias. Expression of *EcMeis2* is absent from the forelimb by TS 8 (Fig. 3I). In the hind limb bud, the strongest expression of *EcMeis2* at this stage is observed in the anterior region of the proximal limb (Fig. 3L). In addition, weaker diffuse expression is present at this stage throughout the hind limb bud. The anterior bias in expression of this gene is particularly surprising, indeed unprecedented, as both its expression and its role in proximal specification are regarded as conserved not just in amniotes but also in developing and regenerating limbs of urodele amphibians (Mercader et al. 2005). This could be explained by redundancy because *Meis1* shares the proximal expression domain and role in proximodistal patterning in both amniotes (Capdevila et al. 1999) and axolotl (Mercader et al. 2005).

Feedback loops between the proximodistal and anterior–posterior axes

A critical feature that coordinates the relative locations and timing of the activities of the AER and ZPA in amniotes is a series of integrated feedback loops between them. The first of these loops to be described is the one between Shh in the ZPA and Fgf expression in the AER (Laufer et al. 1994; Niswander et al. 1994). It was originally described in the context of *Fgf4*, which, as noted above, is not expressed at all in the coquí limb. However, Fgf9 and Fgf17 are also induced by Shh signaling, and the finding in the mouse that either Fgf9 or Fgf17 can act in conjunction with Fgf8 to give proper limb pattern in the absence of Fgf4 (Mariani et al. 2008) suggests that one of these other family members may be acting in the feedback loop in coquí.

Most strikingly, however, two other key genes that integrate Shh and Fgf activity in the developing amniote limb are either not expressed in coquí or expressed in a manner that is not consistent with their critical role in amniotes. Limb morphogenesis in amniotes depends on two interlinked loops that buffer genetic and environmental fluctuations and lead to robust timing and location of Fgf and Shh activity. In the first of these, Shh acts to induce the expression of the Bmp-antagonist Gremlin, which, by interfering with Bmp4

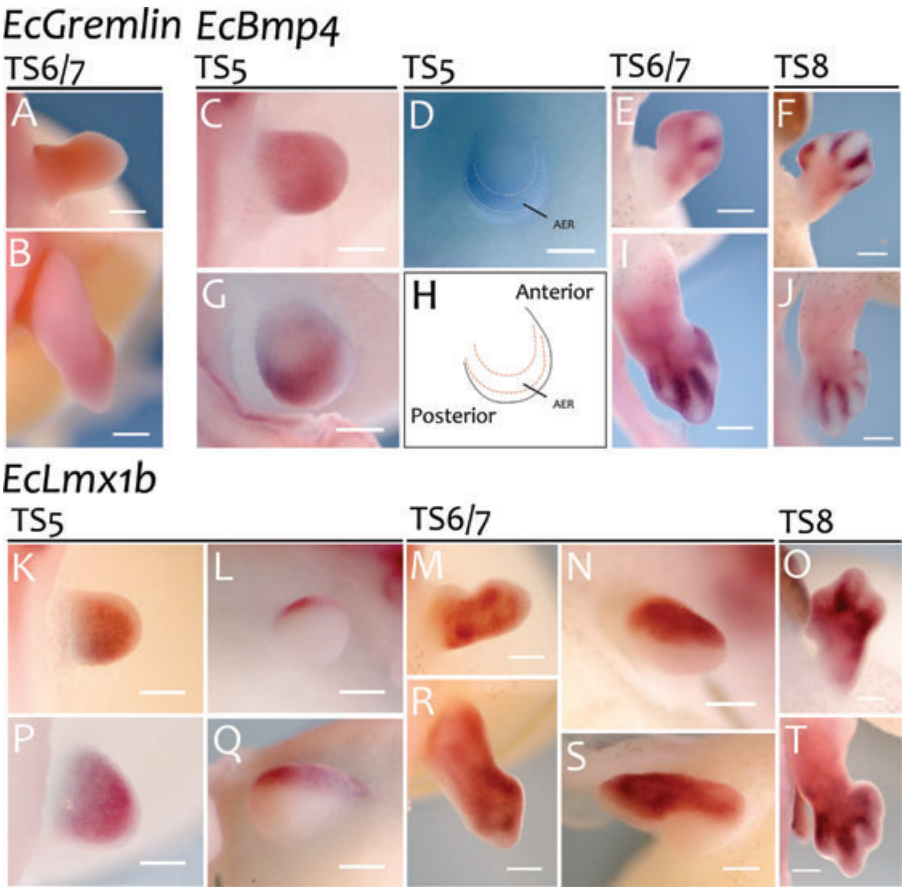

Fig. 4. *EcGremlin*, *EcBmp4*, and *EcLmx1b* expression in coquí limb buds. Expression of *EcGremlin* (A and B) was absent from the embryo through all developmental stages assayed. The expression of *EcBmp4* is diffuse, with stronger expression in the putative AER at TS 5 (C and G). Note the presence of *EcBmp4* within the developing AER (dashed lines in D and H) of the hind limb of a different specimen, viewed from an oblique angle. By TS 6/7, *EcBmp4* begins to resolve in the interdigital mesenchyme (E and I), becoming stronger by TS 8 (F and J). At all stages assayed, the expression of *EcLmx1b* is confined to the dorsal half of the limb bud in both forelimb (K–O) and hind limb (P–T). Forelimbs: A, C, E, F, K–O; hind limbs: B, D, G–J, P–T. Scale = 250 μm.

activity, derepresses ectodermal *Fgf* expression (including *Fgf4*, discussed above), thereby maintaining Shh expression via a positive feedback loop (Capdevila et al. 1999; Zuniga et al. 1999; Michos et al. 2004; Panman et al. 2006). In a second loop, Bmp4 itself upregulates its antagonist, Gremlin (Nissim et al. 2006; Ovchinnikov et al. 2006). The integration of these two loops gives the limb-patterning system its robustness (Benazet et al. 2009). An additional critical aspect of this signaling network is its self-terminating property, wherein the expanding population of cells that at one time express Shh become refractory to activation of Gremlin expression. Eventually, an inhibitory Fgf-Gremlin feedback loop leads to termination of the patterning phase of limb development (Scherz et al. 2004; Verheyden and Sun 2008).

In this context, it is stunning that *EcGremlin*, the key gene that integrates the two feedback loops in the posterior region of the amniote limb bud (Capdevila et al. 1999; Zuniga et al. 1999), is not expressed within any of the developmental stages assayed in coquí limb buds (Fig. 4, A and B). Interestingly, *EcGremlin* shares 74% similarity with a related family member, *Gremlin2* (Table 1; *Ictalurus*). Thus, it is possible that Gremlin2 has adopted the function of Gremlin in coquí embryos, explaining the absence of expression in our study.

To further explore this surprising result, we examined expression of another lynchpin of the two feedback loops, Bmp4, which opposes Shh activity by down-regulating Fgf signaling and both induces and is repressed by Gremlin. Besides an anterior expression in amniote limb buds, *Bmp4* is also expressed throughout the AER (Francis et al. 1994; Yokouchi et al. 1996; Revest et al. 2001). This latter expression domain seems to be conserved, as *EcBmp4* expression in coquí is observed in the "functional" AER (i.e., the domain of *EcFgf8* expression) of both forelimb (Fig. 4C) and hind limb (Fig. 4, G and D, and see schematic in 4H). It is also found in coquí limb bud mesenchyme, although its expression is diffuse throughout the mesoderm and without the anterior bias that would be expected of a gene repressed by an Shh target (Gremlin). Thus, once again, the complex feedback loops that mediate limb patterning in amniotes appear inoperative in coquí. At later stages in amniotes, *Bmp4* expression resolves in the interdigital domains where it is involved in both digit specification (Suzuki et al. 2008) and interdigital apoptosis (Zou and Niswander 1996). These functions

appear to be conserved in coquí, as at TS 6/7 *EcBmp4* expression begins to resolve into the presumptive interdigital mesenchyme (IDM) where initially it is expressed weakly in the forelimb (Fig. 4E) relative to the hind limb (Fig. 4I). By TS 8, expression of *EcBmp4* is strongest within the IDM of the forelimb (Fig. 4F) and is beginning to diminish in the hind limb (Fig. 4J).

The dorsal–ventral axis

In the chicken, the secreted factor Wnt7a is expressed in dorsal ectoderm of the early limb bud, leading to induction of *Lmx1* in distal dorsal mesenchyme (Riddle et al. 1995; Vogel et al. 1995). Lmx1b is an LIM-homeodomain transcription factor that is expressed throughout the dorsal limb mesenchyme, albeit independently of Wnt7a in proximal regions (Parr and McMahon 1998). These genes are both necessary and sufficient for establishing dorsal–ventral pattern in the limb bud. In the absence of Wnt7a, dorsal structures assume a ventralized pattern (Parr and McMahon 1998). Similarly, a ventralized phenotype is seen in mice deficient for *Lmx1b* (Chen et al. 1998), whereas ventral structures can be dorsalized by ectopic *Lmx1b* (Riddle et al. 1995; Vogel et al. 1995). In coquí, expression of *EcLmx1b* is maintained within the dorsal aspect of the developing limb bud throughout early (Fig. 4, K, L, O, and Q), middle (Fig. 4, M, N, R, and D), and late (Fig. 4, O and T) stages. As in amniotes, this dorsal domain of expression represents a distinct boundary between dorsal and ventral halves of the limb, and it is strongly expressed through the latest stages of development assayed in this study in both forelimb and hind limb. In coquí, *EcLmx1b* likely specifies dorsal limb bud cell fate as described for other vertebrates.

In contrast, we were unable to identify a limb bud expression domain for *EcWnt7a* in any region of the embryo at any of the three developmental stages examined (data not shown). It is possible that *EcWnt7a* induces *EcLmx1b* at an earlier stage in coquí. Indeed, in chicken embryos, expression of both *Wnt7a* and *Lmx1b* is strongly detected in the limb primordium well before the limb bud forms (Riddle et al. 1995). Alternatively, a different Wnt may be substituting for Wnt7a activity in the limb bud, just as Wnt3 in the mouse has replaced Wnt3a in the chicken during *Fgf8* and AER induction. In support of this hypothesis, a recent genome survey reveals that *Wnt7a* is absent from the draft genome of *Xenopus tropicalis* (Garriock et al. 2007). Instead, *Wnt7c*, a *Wnt7a*-related gene, is present in *X. tropicalis* at a conserved position (i.e., near an *HDAC* gene) of the original *Wnt7a* locus. This raises the possibility that *Wnt7c* arose in anurans through a gene duplication event involving *Wnt7a*. If true, then Wnt7c may discharge the function of Wnt7a in anuran species, thereby explaining the absence of *Wnt7a* expression during coquí limb development. Finally, it is also possible that whatever Wnt7a-independent mechanism that establishes *Lmx1b* expression in the proximal dorsal limb in amniotes operates throughout the entire dorsal limb bud in coquí.

CONCLUSIONS

The vertebrate limb develops and evolves as a largely modular structure. The identity and expression of the vast majority of genes deployed during limb development remain essentially unchanged among vastly disparate taxa. However, we report important differences in the patterns of spatial or temporal expression, or even the presence, of key factors in *E. coqui*, which may indicate alterations to the molecular signaling mechanisms that underlie limb development in this and related species. These results indicate a surprising evolutionary flexibility in the key regulatory cassettes that coordinate early limb patterning. Nonetheless, use of these core sets of gene networks remains tightly conserved despite significant derived features that are characteristic of coquí frogs, such as direct development. This study sets the stage for comparative molecular analyses of limb development across a wider array of vertebrates, including those such as direct-developing salamanders that converge on similar morphologies or life-history patterns.

Acknowledgments

The authors thank Rick Elinson for generously providing several coquí embryos that were instrumental to the completion of this project. We also thank Gerhard Schlosser for providing a plasmid for probe synthesis of coquí *sonic hedgehog* (*EcShh*; Hanken et al. 2001) and Anne Everly for assistance with animal breeding and husbandry. This work was supported by a grant from the NSF (EF-0334846) to JH, and a grant from the NIH (R37 HD032443) to CJT.

REFERENCES

Barrow, J. R., et al. 2003. Ectodermal *Wnt3/ß-catenin* signaling is required for the establishment and maintenance of the apical ectodermal ridge. *Genes Dev.* 17: 394–409.

Benazet, J. D., et al. 2009. A self-regulatory system of interlinked signaling feedback loops controls mouse limb patterning. *Science* 323: 1050–1053.

Bourgeois, P., et al. 1998. The variable expressivity and incomplete penetrance of the *twist*-null heterozygous mouse phenotype resemble those of Human Saethre-Chotzen syndrome. *Hum. Mol. Genet.* 7: 945–957.

Capdevila, J., Tsukui, T., Rodriquez Esteban, C., Zappavigna, V., and Izpisua Belmonte, J. C. 1999. Control of vertebrate limb outgrowth by the proximal factor *Meis2* and distal antagonism of BMPs by Gremlin. *Mol. Cell* 4: 839–849.

Cecconi, F., Proetzel, G., Alvarez-Bolado, G., Jay, D., and Gruss, P. 1997. Expression of *Meis2*, a *Knotted*-related murine homeobox gene, indicates a role in the differentiation of the forebrain and the somitic mesoderm. *Dev. Dyn.* 210: 184–190.

Chang, W. Y., et al. 2006. Conservation of *Pitx1* expression during amphibian limb morphogenesis. *Biochem. Cell Biol.* 84: 257–262.
Charité, J., McFadden, D. G., and Olson, E. N. 2000. The bHLH transcription factor dHAND controls *Sonic hedgehog* expression and establishment of the zone of polarizing activity during limb development. *Development* 127: 2461–2470.
Chen, H., et al. 1998. Limb and kidney defects in *Lmx1b* mutant mice suggest an involvement of *LMX1B* in Human Nail Patella syndrome. *Nat. Genet.* 19: 51–55.
Christen, B., and Slack, J. M. 1997. *FGF-8* is associated with anteroposterior patterning and limb regeneration in *Xenopus*. *Dev. Biol.* 192: 455–466.
Dealy, C. N., Roth, A., Ferrari, D., Brown, A. M., and Kosher, R. A. 1993. *Wnt-5a* and *Wnt-7a* are expressed in the developing chick limb bud in a manner suggesting roles in pattern formation along the proximodistal and dorsoventral axes. *Mech. Dev.* 43: 175–186.
Dudley, A. T., Ros, M. A., and Tabin, C. J. 2002. A re-examination of proximodistal patterning during vertebrate limb development. *Nature* 418: 539–544.
Dunn, N. R., Winnier, G. E., Hargett, L. K., Schrick, J. J., Fogo, A. B., and Hogan, B. L. 1997. Haploinsufficient phenotypes in *Bmp4* heterozygous null mice and modification by mutations in *Gli3* and *Alx4*. *Dev. Biol.* 188: 235–247.
Elinson, R. P. 1994. Leg development in a frog without a tadpole (*Eleutherodactylus coqui*). *J. Exp. Zool. (Mol. Dev. Evol.)* 270: 202–210.
Elinson, R. P., and Beckham, Y. 2002. Development in frogs with large eggs and the origin of amniotes. *Zoology* 105: 105–117.
Elinson, R. P., Walton, Z., and Nath, K. 2008. *Raldh* expression in embryos of the direct developing frog *Eleutherodactylus coqui* and the conserved retinoic acid requirement for forelimb initiation. *J. Exp. Zool. (Mol. Dev. Evol.)* 310B: 588–595.
Fang, H., and Elinson, R. P. 1996. Patterns of Distal-less gene expression and inductive interactions in the head of the direct developing frog *Eleutherodactylus coqui*. *Dev. Biol.* 179: 160–172.
Fernandez-Teran, M., Piedra, M. E., Kathiriya, I. S., Srivastava, D., Rodriguez-Rey, J. C., and Ros, M. A. 2000. Role of dHAND in the anterior-posterior polarization of the limb bud: implications for the sonic hedgehog pathway. *Development* 127: 2133–2142.
Francis, P. H., Richardson, M. K., Brickell, P. M., and Tickle, C. 1994. Bone morphogenetic proteins and a signalling pathway that controls patterning in the developing chick limb. *Development* 120: 209–218.
Garriock, R. J., Warkman, A. S., Meadows, S. M., D'Agostino, S., and Krieg, P. A. 2007. Census of vertebrate Wnt genes: isolation and developmental expression of *Xenopus* Wnt2, Wnt3, Wnt9a, Wnt9b, Wnt10a, and Wnt16. *Dev. Dyn.* 236: 1249–1258.
Goodrich, L. V., Johnson, R. L., Milenkovic, L., McMahon, J. A., and Scott, M. P. 1996. Conservation of the *hedgehog/patched* signaling pathway from flies to mice: induction of a mouse *patched* gene by Hedgehog. *Genes. Dev.* 10: 301–312.
Hanken, J., et al. 2001. Limb development in a "nonmodel" vertebrate, the direct-developing frog *Eleutherodactylus coqui*. *J. Exp. Zool. (Mol. Dev. Evol.)* 291: 375–388.
Kawakami, Y., Wada, N., Nishimatsu, S. I., Ishikawa, T., Noji, S., and Nohno, T. 1999. Involvement of *Wnt-5a* in chondrogenic pattern formation in the chick limb bud. *Dev. Growth Differ.* 41: 29–40.
Kengaku, M., et al. 1998. Distinct WNT pathways regulating AER formation and dorsoventral polarity in the chick limb bud. *Science* 280: 1274–1277.
Kerney, R., and Hanken, J. 2008. Gene expression reveals unique skeletal patterning in the limb of the direct-developing frog, *Eleutherodactylus coqui*. *Evol. Dev.* 10: 439–448.
Laufer, E., Nelson, C. E., Johnson, R. L., Morgan, B. A., and Tabin, C. 1994. *Sonic hedgehog* and *Fgf-4* act through a signaling cascade and feedback loop to integrate growth and patterning of the developing limb bud. *Cell* 79: 993–1003.
Lewandoski, M., Sun, X., and Martin, G. R. 2000. Fgf8 signalling from the AER is essential for normal limb development. *Nat. Genet.* 26: 460–463.
Logan, M., and Tabin, C. J. 1999. Role of Pitx1 upstream of Tbx4 in specification of hindlimb identity. *Science* 283: 1736–1739.
Mariani, F. V., Ahn, C. P., and Martin, G. R. 2008. Genetic evidence that FGFs have an instructive role in limb proximal-distal patterning. *Nature* 453: 401–405.
Marigo, V., Davey, R. A., Zuo, Y., Cunningham, J. M., and Tabin, C. J. 1996a. Biochemical evidence that Patched is the Hedgehog receptor. *Nature* 384: 176–179.
Marigo, V., Laufer, E., Nelson, C. E., Riddle, R. D., Johnson, R. L., and Tabin, C. 1996b. Sonic Hedgehog regulates patterning in early embryos. *Biochem. Soc. Symp.* 62: 51–60.
Marigo, V., Scott, M. P., Johnson, R. L., Goodrich, L. V., and Tabin, C. J. 1996c. Conservation in *hedgehog* signaling: induction of a chicken *patched* homolog by *Sonic hedgehog* in the developing limb. *Development* 122: 1225–1233.
McFadden, D. G., McAnally, J., Richardson, J. A., Charité, J., and Olson, E. N. 2002. Misexpression of dHAND induces ectopic digits in the developing limb bud in the absence of direct DNA binding. *Development* 129: 3077–3088.
Mercader, N., et al. 1999. Conserved regulation of proximodistal limb axis development by Meis1/Hth. *Nature* 402: 425–429.
Mercader, N., et al. 2000. Opposing RA and FGF signals control proximodistal vertebrate limb development through regulation of Meis genes. *Development* 127: 3961–3970.
Mercader, N., Tanaka, E. M., and Torres, M. 2005. Proximodistal identity during vertebrate limb regeneration is regulated by Meis homeodomain proteins. *Development* 132: 4131–4142.
Michos, O., Panman, L., Vintersten, K., Beier, K., Zeller, R., and Zuniga, A. 2004. *Gremlin*-mediated BMP antagonism induces the epithelial-mesenchymal feedback signaling controlling metanephric kidney and limb organogenesis. *Development* 131: 3401–3410.
Nissim, S., Hasso, S. M., Fallon, J. F., and Tabin, C. J. 2006. Regulation of *Gremlin* expression in the posterior limb bud. *Dev. Biol.* 299: 12–21.
Niswander, L., Jeffrey, S., Martin, G. R., and Tickle, C. 1994. A positive feedback loop coordinates growth and patterning in the vertebrate limb. *Nature* 371: 609–612.
Ovchinnikov, D. A., et al. 2006. BMP receptor type IA in limb bud mesenchyme regulates distal outgrowth and patterning. *Dev. Biol.* 295: 103–115.
Panganiban, G., et al. 1997. The origin and evolution of animal appendages. *Proc. Natl. Acad. Sci. USA* 94: 5162–5166.
Panman, L., et al. 2006. Differential regulation of gene expression in the digit forming area of the mouse limb bud by SHH and Gremlin 1/FGF-mediated epithelial-mesenchymal signalling. *Development* 133: 3419–3428.
Parr, B. A., and McMahon, A. P. 1998. Sexually dimorphic development of the mammalian reproductive tract requires *Wnt-7a*. *Nature* 395: 707–710.
Qu, S., et al. 1997. Polydactyly and ectopic ZPA formation in *Alx-4* mutant mice. *Development* 124: 3999–4008.
Qu, S., Tucker, S. C., Zhao, Q., deCrombrugghe, B., and Wisdom, R. 1999. Physical and genetic interactions between *Alx4* and *Cart1*. *Development* 126: 359–369.
Revest, J. M., Spencer-Dene, B., Kerr, K., De Moerlooze, L., Rosewell, I., and Dickson, C. 2001. Fibroblast growth factor receptor 2-IIIb acts upstream of *Shh* and *Fgf4* and is required for limb bud maintenance but not for the induction of *Fgf8*, *Fgf10*, *Msx1*, or *Bmp4*. *Dev. Biol.* 231: 47–62.
Richardson, M. K., Carl, T. F., Hanken, J., Elinson, R. P., Cope, C., and Bagley, P. 1998. Limb development and evolution: a frog embryo with no apical ectodermal ridge (AER). *J. Anat.* 192: 379–390.
Riddle, R. D., Ensini, M., Nelson, C., Tsuchida, T., Jessell, T. M., and Tabin, C. 1995. Induction of the LIM homeobox gene *Lmx1* by WNT7a establishes dorsoventral pattern in the vertebrate limb. *Cell* 83: 631–640.
Riddle, R. D., Johnson, R. L., Laufer, E., and Tabin, C. 1993. *Sonic hedgehog* mediates the polarizing activity of the ZPA. *Cell* 75: 1401–1416.

Rose, T. M., Henikoff, J. G., and Henikoff, S. 2003. CODEHOP (COnsensus-DEgenerate Hybrid Oligonucleotide Primer) PCR primer design. *Nucleic Acids Res.* 31: 3763–3766.

Sabo, M. C., Nath, K., and Elinson, R. P. 2009. *Lbx1* expression and frog limb development. *Dev. Genes Evol.* 219: 609–612.

Scherz, P. J., Harfe, B. D., McMahon, A. P., and Tabin, C. J. 2004. The limb bud Shh-Fgf feedback loop is terminated by expansion of former ZPA cells. *Science* 305: 396–399.

Schlosser, G. 2001. Using heterochrony plots to detect the dissociated coevolution of characters. *J. Exp. Zool. (Mol. Dev. Evol.)* 291: 282–304.

Stone, D. M., et al. 1996. The tumour-suppressor gene *patched* encodes a candidate receptor for Sonic hedgehog. *Nature* 384: 129–134.

Sun, X., Lewandoski, M., Meyers, E. N., Liu, Y. H., Maxson, R. E., Jr., and Martin, G. R., 2000. Conditional inactivation of *Fgf4* reveals complexity of signalling during limb bud development. *Nat. Genet.* 25: 83–86.

Suzuki, T., Hasso, S. M., and Fallon, J. F. 2008. Unique SMAD1/5/8 activity at the phalanx-forming region determines digit identity. *Proc. Natl. Acad. Sci. USA* 105: 4185–4190.

Suzuki, T., Takeuchi, J., Koshiba-Takeuchi, K., and Ogura, T. 2004. *Tbx* genes specify posterior digit identity through Shh and BMP signaling. *Dev. Cell* 6: 43–53.

te Welscher, P., Fernandez-Teran, M., Ros, M. A., and Zeller, R. 2002. Mutual genetic antagonism involving GLI3 and dHAND prepatterns the vertebrate limb bud mesenchyme prior to SHH signaling. *Genes Dev.* 16: 421–426.

Townsend, D. S., and Stewart, M. M. 1985. Direct development in *Eleutherodactylus coqui* (Anura: Leptodactylidae): a staging table. *Copeia* 1985: 423–436.

Verheyden, J. M., and Sun, X. 2008. An *Fgf/Gremlin* inhibitory feedback loop triggers termination of limb bud outgrowth. *Nature* 454: 638–641.

Vogel, A., Rodriguez, C., Warnken, W., and Izpisua Belmonte, J. C. 1995. Dorsal cell fate specified by chick *Lmx1* during vertebrate limb development. *Nature* 378: 716–720.

Yamaguchi, T. P., Bradley, A., McMahon, A. P., and Jones, S. 1999. A *Wnt5a* pathway underlies outgrowth of multiple structures in the vertebrate embryo. *Development* 126: 1211–1223.

Yokouchi, Y., et al. 1996. BMP-2/-4 mediate programmed cell death in chicken limb buds. *Development* 122: 3725–3734.

Zakany, J., and Duboule, D. 1996. Synpolydactyly in mice with a targeted deficiency in the *HoxD* complex. *Nature* 384: 69–71.

Zhang, Z., Verheyden, J. M., Hassell, J. A., and Sun, X. 2009. FGF-regulated Etv genes are essential for repressing *Shh* expression in mouse limb buds. *Dev. Cell* 16: 607–613.

Zou, H., and Niswander, L. 1996. Requirement for BMP signaling in interdigital apoptosis and scale formation. *Science* 272: 738–741.

Zuniga, A., Haramis, A. P., McMahon, A. P., and Zeller, R. 1999. Signal relay by BMP antagonism controls the SHH/FGF4 feedback loop in vertebrate limb buds. *Nature* 401: 598–602.